A11102 696831
NBS
PUBLICATIONS

NBSIR 87-3572

Diffusion-Controlled Reaction in a Vortex Field

Ronald G. Rehm, Howard R. Baum
and Daniel W. Lozier

U.S. DEPARTMENT OF COMMERCE
National Bureau of Standards
Center for Applied Mathematics and
Center for Fire Research
Gaithersburg, MD 20899

June 1987

U.S. DEPARTMENT OF COMMERCE
NATIONAL BUREAU OF STANDARDS

QC
100
.U56
#87-3572
1987
C.2

Research Information Center
National Bureau of Standards
Gaithersburg, Maryland 20899

NBSC
QC100
.U56
NO.87-3572
1987
C.2

NBSIR 87-3572

DIFFUSION-CONTROLLED REACTION IN A VORTEX FIELD

Ronald G. Rehm, Howard R. Baum
and Daniel W. Lozier

U.S. DEPARTMENT OF COMMERCE
National Bureau of Standards
Center for Applied Mathematics and
Center for Fire Research
Gaithersburg, MD 20899

June 1987

U.S. DEPARTMENT OF COMMERCE, Malcolm Baldrige, *Secretary*
NATIONAL BUREAU OF STANDARDS, Ernest Ambler, *Director*

Diffusion-Controlled Reaction in a Vortex Field

Ronald G. Rehm,* Howard R. Baum† and Daniel W. Lozier‡
National Bureau of Standards
Gaithersburg, MD 20899

June 4, 1987

Abstract

A two-dimensional model of a constant-density diffusion-controlled reaction between unmixed species initially occupying adjacent half-spaces is formulated and analyzed. An axisymmetric viscous vortex field satisfying the Navier-Stokes equations winds up the interface between the species as they diffuse together and react. A flame-sheet approximation of the rapid reaction is made using Shvab-Zeldovich dependent variables. The model was originally proposed by F. Marble, who performed a local analysis and determined the total consumption rate along the flame sheet. The present paper describes a global similarity solution to the problem which is Fourier analyzed in a Lagrangian coordinate system. An asymptotic analysis of the Fourier amplitudes, valid for large Schmidt numbers is presented. The solution is evaluated numerically in Lagrangian and Eulerian coordinate systems. This problem has been studied as part of a more general model which has application to the description of turbulent combustion.

---

*Center for Applied Mathematics

†Center for Fire Research

‡Center for Applied Mathematics

1 Introduction

The theoretical study of chemical reactions in complex flow fields, for example turbulent reacting flows, has received increased attention lately [1]-[8]. This attention is warranted not only because numerical and analytical progress is being made in addressing the problem, but also because a much clearer physical picture of turbulent flows and their coupling to combustion processes has been achieved through experiments over the past fifteen years [9]-[12]. Turbulent combustion is difficult to analyze because it is highly nonlinear, transient and involves a wide range of length and time scales. When the Reynolds number is large, experiments indicate that the length and time scales associated with turbulent combustion can be separated by phenomenon into large and small scales. The large, or geometrical, scale is essentially inviscid or nondissipative and is related to the geometry defining the flow configuration and the fuel and oxidizer distributions. Combustion, on the other hand, takes place on the small scale associated with the diffusion of fuel and oxidizer into each other; it "rides on" the geometrical scale and establishes the rate at which the reactants disappear and heat is released.

An outline of a general approach for studying the problem of turbulent reacting flows, based on these observations and using both analytical and numerical methods, is given in a recent paper by Baum, Corley and Rehm [13]. The approach is to analyze large-scale flow fields separately from the small-scale mixing and reaction using the observation that these processes occur on widely differing length and time scales for large Reynolds numbers. The component problems are treated individually, but in a way that will allow the phenomena to be coupled through analytical and computational techniques. Mathematical analysis is used extensively; however, the task is ultimately computational, and computations must be carried out for any configuration of practical interest.

Also presented in [13] is a model for three-dimensional small-scale mixing and reaction in a stretched vortex flow field; this model includes the critical features for turbulent combustion of flame stretching and the three-dimensional effect of vortex stretching. In [14], Marble originally posed a similar but more specialized two-dimensional model problem of small-scale

mixing and reaction and studied it analytically. His model includes the two-dimensional effect of flame stretching, and was analyzed using methods presented earlier by Carrier, Fendell and Marble [15] locally along the flame front to provide global dependences of the fuel and oxidizer consumption rates upon the governing parameters. The Marble problem has several important features: it is a diffusion-controlled reaction in a viscously spreading vorticity field which stretches the flame sheet. Even though it is only two dimensional, it approximates chemical reactions in individual vortices which occur in shear-layer mixing experiments, such as those of Mungal and Dimotakis [11]. Generalizations of the Marble problem for a stretched vortex flow field and for reactions which release heat, using a local analysis, have been performed by Karagozian [23] and Karagozian and Marble [24]. We analyze the Marble problem in a manner very different from that described in the original paper of Marble [14].

Two-dimensional numerical computations of the flow properties in reacting mixing layers have recently been carried out [16]-[20]. In these computations and the experiments they simulate, two fluids, one containing fuel and the other containing oxidizer and each flowing unidirectionally with its own velocity are brought into contact at a "splitter plate". Downstream of the point of contact, the two fluids mix and chemical reactions take place as they diffuse together. Experiments indicate that during the early stages of development of these mixing layers, the flow fields remain primarily two dimensional. Then, before vortex pairing begins, the Marble problem can be regarded as an analytical approximation to combustion in one of the vortices. Also, recently, a direct numerical computation of the Marble problem has been undertaken by Laverdant and Candel [21]. All of these computations demonstrate that, even for the small-scale problem of mixing, diffusion and reaction, without attempting to calculate large-scale flow fields also, the computations are large, complex and difficult.

The work presented in this paper is essentially analytical, and, within the context of the mathematical model, permits one to calculate combustion properties much more accurately for given computational resources than direct numerical solution. Therefore, it could be used, for example, to test the accuracy of the numerical computations cited above. The novel features of our work compared with that of Marble [14] are (i) it is observed that

the convection-diffusion equation for the Shvab-Zeldovich variable permits a similarity solution, reducing the number of independent variables from three (radius, angle and time) to two (angle and similarity variable); (ii) as in [13], a Lagrangian coordinate system is used to eliminate flame-sheet resolution problems induced by vortex winding; (iii) Fourier analysis in angle and a combined numerical and analytical treatment in the similarity variable allow one to solve the global problem essentially exactly. The solution to this problem will provide a special case on which to test methods for solution to the more general problems described in [13].

In Section 2 we formulate the problem and give its complete mathematical description. Special cases of the general problem are presented and solved in Section 3. In this section an approximate solution for large Schmidt number is given which is particularly valuable because it displays the analytical behavior of the problem. It is also appropriate for diffusion controlled reactions in many miscible liquids where the Schmidt number really is large. Results calculated both from the special cases and more general numerical methods are given in Section 4. In Section 5 we calculate the global fuel and oxidizer consumption rates using the large Schmidt number analytical result and assuming in addition that the Reynolds number is large. Finally, in Section 6, some conclusions are drawn from this study.

2 Formulation of the Problem

Consider the model in which initially there is fuel in the left half-plane and oxidizer in the right half-plane in arbitrary proportions. These half-spaces are brought into contact and simultaneously a line vortex with axis at the origin is imposed (see Figure 1). The vortex induces a convective mixing of the interface between the two species, increasing the area of the separating surface in the neighborhood of the origin and enhancing the diffusion of the species into each other. It is assumed that the reaction rate is sufficiently rapid for the process to be limited by diffusion, and a flame-sheet approximation is made for the reaction. The chemical reaction is assumed to take place at constant density and all diffusion coefficients (kinematic viscosity, thermal and concentration coefficients) are assumed

to be constant. The tangential velocity v_θ imposed is

$$v_\theta(r,t) = r\frac{d\theta}{dt} = \frac{\Gamma}{2\pi r}[1-\exp(-\eta)] \tag{1}$$

where Γ is the circulation of the vortex, ν is the kinematic viscosity and $\eta = r^2/4\nu t$ is a similarity variable.

With the assumptions described above, the equations for species and energy are decoupled from the momentum and continuity equations; they are equations representing a balance between convection, diffusion and reaction. The reaction rate, which is very nonlinear in concentrations and temperature in general, can be eliminated by taking a linear combination of the dependent variables when the additional assumption is made that the thermal and species diffusion coefficients are equal. This is a common procedure in the theoretical analysis of combustion equations [2]. The linear combinations are often called coupling functions or Shvab-Zeldovich variables, and in this case all satisfy the same equation; therefore, one need only solve for one dependent variable.

The Shvab-Zeldovich variable Z satisfies the convection-diffusion equation

$$\frac{\partial Z}{\partial t} + \frac{v_\theta}{r}\frac{\partial Z}{\partial \theta} = D\left(\frac{\partial^2 Z}{\partial r^2} + \frac{1}{r}\frac{\partial Z}{\partial r} + \frac{1}{r^2}\frac{\partial^2 Z}{\partial \theta^2}\right) \tag{2}$$

where D is the species diffusion coefficient, assumed to be constant and the same for each species. The initial conditions are that $Z = 1$ for $\pi/2 \le \theta \le 3\pi/2$ and $Z = 0$ for $-\pi/2 \le \theta \le \pi/2$.

Integrating the tangential velocity gives the angle $\theta(r,\theta_0,t)$ at time t for any fluid element initially located at r,θ_0 . A change of variables to the Lagrangian coordinates, ρ,θ_0,τ,

$$\begin{aligned} r &= \rho \\ \theta &= \theta_0 + \frac{\Gamma}{8\pi\nu}\frac{1-E_2(\eta)}{\eta} \\ t &= \tau \end{aligned} \tag{3}$$

where $E_j(z) = \int_1^\infty t^{-j}\exp(-zt)dt$, can then be made in the equation for Z. Finally, assuming that Z is only a function of the similarity variable η and

the angle θ_0, and performing a Fourier decomposition in the angle,

$$Z(\eta, \theta_0) = \sum_{n=-\infty}^{\infty} Z_n(\eta) \exp(in\theta_0) \tag{4}$$

a system of equations for each of the Fourier mode amplitudes Z_n is obtained:

$$\frac{d^2 Z_n}{d\eta^2} + f_n(\eta)\frac{dZ_n}{d\eta} + g_n(\eta) Z_n = 0 \tag{5}$$

where

$$f_n(\eta) = \mathrm{Sc} + \frac{1}{\eta} + in\frac{1 - \exp(-\eta)}{\eta^2}\,\mathrm{Re}$$

$$g_n(\eta) = -\left(\left[\frac{1 - \exp(-\eta)}{\eta}\,\mathrm{Re}\right]^2 + 1\right)\frac{n^2}{4\eta^2}$$
$$+\frac{in}{2}\frac{\exp(-\eta) - [(1 - \exp(-\eta))/\eta]}{\eta^2}\,\mathrm{Re}$$

and where $\mathrm{Sc} = \nu/D$ is the Schmidt number and $\mathrm{Re} = \Gamma/4\pi\nu$ is the Reynolds number based upon the circulation Γ.

This equation is an ordinary differential equation for Z_n in the similarity variable η . Boundary conditions are that the solution remain bounded as η goes to zero and that the initial conditions on Z_n are recovered as η goes to infinity. From the symmetry of the problem, the initial conditions are found to be, for even values of n, $Z_n(\eta \to \infty) = 0$, and for odd values of $n = 2m + 1$,

$$Z_{2m+1}(\eta \to \infty) = \frac{(-1)^{m+1}}{\pi}\frac{1}{2m+1} \tag{6}$$

For computation, the infinite endpoint is replaced by a finite parameter.

A very special case discussed in more detail in Section 3.2 can be used to test the numerical methodology and the computer programming. It also allows us to determine the boundary conditions in the similarity variable from initial conditions in the original variables. It is the pure diffusion case, which arises when the circulation Γ is taken to be zero. The known solution

for the diffusion of two half-spaces into each other is given in terms of an error function, which is expressed in cylindrical coordinates and Fourier analyzed to give Z_n in terms of Bessel functions. This result has been used to examine the sensitivity of the numerical solution to the finite truncation of the infinite interval, to the number of terms retained in the Fourier synthesis of Z, and to the mesh size used in the solution of the two point boundary value problem, Eq.(5).

The general solution for $Z_n(\eta)$ is a complex-valued function of the real variable η. From the governing equation, it is seen that $Z_{-n}(\eta)$ is the complex conjugate of $Z_n(\eta)$. The modes Z_n are synthesized using an FFT routine to determine $Z(\eta, \theta_0)$, and information about the location of the flame-sheet and the rate at which fuel is consumed can be determined.

3 Solutions

3.1 Small Circulation

When Re $= 0$, the problem reduces to the simple one of a diffusing, reacting interface; fuel in the left half-space and oxidizer in the right half-space diffuse into each other and react. For this problem, the Shvab-Zeldovich variable $Z_0(\eta, \theta_0)$ is given by

$$Z_0(\eta, \theta_0) = (1/2)\,\mathrm{erfc}\,(\sqrt{\mathrm{Sc}\,\eta}\cos\theta_0) \tag{7}$$

In this case the Eulerian and Lagrangian coordinates are the same. Fourier analysis yields

$$Z_0(\eta, \theta_0) = A_0 + 2\sum_{m=0}^{\infty} A_{2m+1}(\eta)\cos[(2m+1)\theta_0] \tag{8}$$

where $A_0 = 1/2$ and

$$A_{2m+1}(\eta) = \frac{(-1)^{m+1}}{\sqrt{2\pi}}\frac{1}{2m+1}\sqrt{\mathrm{Sc}\,\eta/2}\exp(-\mathrm{Sc}\,\eta/2) \\ [I_m(\mathrm{Sc}\,\eta/2) + I_{m+1}(\mathrm{Sc}\,\eta/2)] \tag{9}$$

The amplitudes $A_{2m+1}(\eta)$ satisfy

$$\frac{d^2 A_{2m+1}}{d\eta^2} + (\mathrm{Sc} + \frac{1}{\eta})\frac{dA_{2m+1}}{d\eta} - \frac{(2m+1)^2}{4\eta^2} A_{2m+1} = 0 \qquad (10)$$

Compare Eq.(5) with $\mathrm{Re} = 0$ and $n = 2m + 1$. The symmetry of the problem implies that all even Fourier modes are zero.

Boundary conditions for Eq.(10) are determined from the Fourier expansion of the diffusion solution when $\eta \to \infty$. These boundary conditions are simply the initial conditions for the pure diffusion problem; for a finite value of radius r, $\eta \to \infty$ as $t \to 0$. Hence in Eq.(7) for $0 \leq \theta_0 \leq 2\pi$

$$Z(\eta \to \infty, \theta_0) = H(\theta_0 - \pi/2) - H(\theta_0 - 3\pi/2) \qquad (11)$$

where $H(x)$ is the Heaviside function of x. Fourier analysis of $Z(\infty, \theta_0)$ provides the boundary values for $A_{2m+1}(\eta)$ as $\eta \to \infty$: $A_0 = 1/2$ and

$$A_{2m+1}(\eta \to \infty) = \frac{(-1)^{m+1}}{\pi} \frac{1}{2m+1} \qquad (12)$$

Note that the boundary conditions for the pure diffusion problem in terms of the similarity variable are also the boundary conditions for the general Marble problem, since the initial conditions for both problems are the same.

The solution given by Eq.(8) and Eq.(9) have been used as the base state for a perturbation analysis when the Reynolds number is small. Only odd modes need be considered, and since Fourier modes of negative integer n are the complex conjugate of the corresponding Fourier mode of positive integer, only Fourier components with positive integers need be considered. Comparison between results obtained by this technique and results obtained by direct numerical computation of the mode amplitudes using a tridiagonal solver affords a useful check on the numerical procedure used to solve Eq.(5). We have achieved agreement to three significant figures for $\mathrm{Re} = 0.1$ and $\mathrm{Sc} = 1$.

3.2 Large Schmidt Number

When the Schmidt number is infinite, diffusion is unimportant and Eq.(2) is purely a convection equation in which the change of variables to Lagrangian

coordinates reduces the problem to a trivial one. When the Schmidt number is large, asymptotic methods allow one to determine an approximate analytical solution to Eq.(5) from which the character of the solution to Eq.(2) for large Reynolds number can be determined. A change of dependent variable to $W_n(\eta)$ where

$$Z_n(\eta) = W_n(\eta) \exp\left(-\operatorname{Sc}\eta/2 - \ln\eta/2 - (in\operatorname{Re}/2)[E_2(\eta) - 1]/\eta\right) \tag{13}$$

gives the equation

$$\frac{d^2W_n}{d\eta^2} + F_n(\eta;\operatorname{Re},\operatorname{Sc})W_n(\eta) = 0 \tag{14}$$

where

$$F_n(\eta;\operatorname{Re},\operatorname{Sc}) = \frac{-(n^2/2-1)}{2\eta^2} - \frac{(\operatorname{Sc}+1/\eta)^2}{4} - \frac{in\operatorname{Re}\operatorname{Sc}}{2}\frac{(1-e^{-\eta})}{\eta^2} \tag{15}$$

A singular perturbation analysis of Eq.(14) for large Sc yields two solutions $W_n^+(\eta)$ and $W_n^-(\eta)$, of which the former grows exponentially for large η, and the latter decays. The solutions, in turn, imply that the corresponding solutions $Z_n^+(\eta), Z_n^-(\eta)$ become constant and decay exponentially for large η. Since the desired solution to Eq.(2) must pass to the pure-diffusion case for large η, we have

$$Z_{2m+1}^+(\eta \to \infty) \to \frac{(-1)^{m+1}}{\pi(2m+1)} \tag{16}$$

and the constant multiple of $Z_{2m+1}^+(\eta)$ is determined. Since $Z_{2m+1}^-(\eta)$ decays exponentially as $\eta \to \infty$, any multiple of $Z_{2m+1}^-(\eta)$ can be added and we still have a solution. However, the solution for $Z_{2m+1}(\eta)$ must be bounded as $\eta \to 0$, and this fixes a linear combination of Z_{2m+1}^+ and Z_{2m+1}^-. Examination of Z_{2m+1}^+ to leading order in Sc shows that it is a constant throughout while the other solution is singular at $\eta = 0$ in the limit as $\operatorname{Sc} \to \infty$. Hence it is the desired solution!

Carrying out the asymptotic analysis for large Sc to next order yields

$$Z_{2m+1}^+(\eta) \cong \frac{(-1)^{m+1}}{\pi(2m+1)} \exp\left[\frac{-(2m+1)^2}{4\operatorname{Sc}\eta}(A - iB)\right] \tag{17}$$

where

$$A = 1 + \frac{\mathrm{Re}^2}{\eta^2}\left[\frac{1}{3} - 2E_4(\eta) + E_4(2\eta)\right]$$
$$B = \frac{2\,\mathrm{Re}}{2m+1}\left[\frac{-1}{2\eta} + \frac{E_3(\eta)}{\eta} + E_2(\eta)\right]$$

Two observations can be made about this asymptotic expression. First, as $\mathrm{Sc} \to \infty$, the argument of the exponential goes to zero and $Z^+_{2m+1}(\eta)$ goes to the appropriate constant, namely $(-1)^{m+1}/[2\pi(2m+1)]$. Second, for small η, $Z^+_{2m+1}(\eta)$ goes to zero as $\exp[-const./\eta]$.

Substitution of Eq.(17) into Eq.(4) and performing some simplification yields the approximate solution to Eq.(2) for large Schmidt number:

$$\tilde{Z}(\eta, \theta_0) = 1/2 + 2\sum_{m=0}^{\infty} \frac{\exp[-\tilde{A}_m(\eta)]}{\pi(2m+1)} \sin[(2m+1)\Phi_0] \qquad (18)$$

where

$$\tilde{A}_m(\eta;\, \mathrm{Re}\,,\, \mathrm{Sc}\,) = (2m+1)^2 \frac{1 + \mathrm{Re}^2 \tilde{f}_1(\eta)}{4\,\mathrm{Sc}\,\eta}$$
$$\Phi_0 = \theta_0 \mp \frac{\pi}{2} - \frac{\mathrm{Re}}{2\,\mathrm{Sc}} \tilde{f}_2(\eta) \qquad (19)$$

and where

$$\tilde{f}_1(\eta) = [1/3 - 2E_4(\eta) + E_4(2\eta)]/\eta^2$$
$$\tilde{f}_2(\eta) = [(E_3(\eta) - 1/2)/\eta + E_2(\eta)]/\eta$$

Plots of functions $\tilde{f}_1$ and $\tilde{f}_2$ are shown in Figures 2a and 2b; they are rather smooth functions which allow us to determine the analytical behavior of $\tilde{Z}$ for large Schmidt numbers. For small η, $\tilde{f}_1 \to 1$ and $\tilde{f}_2 \to (1/2)\ln\eta$. For large η, $\tilde{f}_1 \to 1/(3\eta^2)$ and $\tilde{f}_2 \to -1/(2\eta)$.

Some important and illuminating observations can be made from the asymptotic solution Eq.(18). First, note that $\tilde{Z} - 1/2$ is a Fourier sine series. When the sum of the terms in this series is small, the solution for the Shvab- Zeldovich variable is approximately $1/2$. Since, for a stoichiometric mixture, $Z = 1/2$ is the equation for the flame sheet, the flame sheet for

such a mixture occurs near where the sum of the Fourier series is small. Now, all terms of the series are exactly zero when $\Phi_0 = 0$, and this condition determines the equation for the flame sheet $\theta_0(\eta)$ for a stoichiometric mixture. However, the terms in the series will also be small when the argument of the exponential is large, and, when the Reynolds number is large, this occurs provided η is not too large.

The physical interpretation of these mathematical statements for large Reynolds and Schmidt numbers is as follows. For a stoichiometric mixture, there are two reaction regions. In the outer region there is a flame sheet, which remains close to the convectively mixed interface in the absence of diffusion. This interface is determined by the equation $\Phi_0 = 0$, and for moderately large η, is very close to $\theta_0 = \pm\pi/2$, which are the equations for the initial interface in the Lagrangian coordinate system. In the inner region, there is a burnt core in which both fuel and oxidizer are depleted, and the growth of this core is determined by the condition that the arguments of the exponentials are large enough that each of the terms in the Fourier series is negligible. For a large Reynolds number (and Schmidt number) this condition determines a value of the similarity variable, η^* say, and the growth of the burnt core is determined then by the equation $r^2/4\nu t = \eta^*$. The observations about the burnt core are consistent with those made by Marble and Karagozian [14], [23], [24].

3.3 Special Cases

Two special cases provide insight into the interplay between the analysis and the physics and give limiting cases against which to check calculated results. The first case is that for which a solution is provided in Subsection 3.1, namely the pure diffusion case. Here, no vorticity is present so that $\Gamma = 0$ and $\mathrm{Re} = 0$. In Figure 3 the solution for this case is shown; contours of constant amplitude Z are shown in either a Lagrangian or an Eulerian coordinate system, since when $\mathrm{Re} = 0$ both coordinate systems are the same (essentially θ_o and the square root of η). The plot is not shown all the way to the origin for technical reasons and only goes out to the square root of ten, which is related to the value used to truncate the infinite interval in the similarity variable. The flame sheet is located along any one

of these constant-amplitude contours, depending upon the concentrations of fuel and oxidizer initially in each half space; for a stoichiometric mixture initially, the contour $Z = 1/2$ is where the flame sheet resides. Since this case is for pure diffusion, the contours should be straight lines (distorted here by the plotting routines); Z varies in a one-dimensional manner from its value of one in the left half-plane to zero in the right half-plane. The contours for which $Z > 1/2$ are shown as solid lines, whereas the countours for which $Z < 1/2$ are shown as dashed lines.

The second simple case to calculate and to physically interpret is that in which there is no diffusion, i.e., $D = 0$ and therefore $\mathrm{Sc} = \infty$. In this case Eq.(2) becomes purely a convective equation, which is solved by the Lagrangian to Eulerian coordinate system transformation, Eq.(4). In Figure 4 are shown plots of the interface for four values of the Reynolds number $\mathrm{Re} = \Gamma/(4\pi\nu) = 2, 4, 6$ and 8. Two points should be emphasized about this figure. First, these plots do not represent the time evolution or convective mixing of a particular instance of the problem, even though the sequence gives this illusion. Second, the time evolution of any one example of the problem, i.e., one Reynolds number, can be visualized as follows. The interface shape is a curve or functional relation between θ and η, and any location on this interface is given by a specific pair η, θ. Since $\eta = r^2/4\nu t$, a particular location on the interface at one time t will determine a radial position r. At a later time, the interface shape does not change and this location will "diffuse" out to a new radial position determined by the condition that η remains constant. Therefore, the interface will retain the same shape, determined by the η, θ relation as time increases, but the length scale characterizing the interface will increase as $r \propto \sqrt{t}$.

3.4 Numerical Results

The solution given by Eq.(7) and that given by Eqs.(8) and (9) are for pure diffusion and can test the numerical methodology used to solve the ordinary differential equations (5) and the FFT procedures needed for the solution for $Z(\eta, \theta_0)$. Numerical solution of Eq.(5) has been performed for many values of the parameters Re and Sc using a central difference approximation to the differential operators. The interval of integration for

the differential equation is truncated to carry out the numerical integration and asymptotic values for the Fourier amplitudes are applied at the truncated location. A finite number of Fourier modes has been computed, and, as noted above, only odd modes of integer greater than zero have been computed. The analytical behavior of the solution for small values of the independent variable η must be handled carefully for lower order modes; therefore, a different dependent variable is computed near the origin. The pure diffusion case, when $Re = 0$, has been used to assess accuracy, particularly the effects of the finite truncation value, the number of Fourier modes and the number of grid points in the finite difference scheme required for a specified resolution.

In Figure 5 there are four mode amplitudes displayed, modes 1, 3, 5, and 7, as functions of the similarity variable η for Reynolds number zero and Schmidt number one. Mode 1 is in the upper left corner, mode 3 is in the upper right corner, mode 5 is in the lower left corner and mode 7 is in the lower right corner. In each case the solid line is the real part of the mode amplitude, the dashed line is the imaginary part and the asterisks line is the modulus. Since this is the pure diffusion case, the amplitudes are real functions. For this calculation, 99 integration nodes and 15 Fourier modes were used, and the dependent variable was changed at $\eta = 1$. Each of the amplitudes should asymptote for large values of the independent variable η; the truncation value of η has been taken as ten. From the figure it can be seen that modes 1,3 and 5 seem to be asymptoting, but that mode 7 is still growing at $\eta = 10$. However, it should also be noted that the magnitude of mode 7 is at least an order of magnitude smaller than that of mode 1.

In Figure 3, shown in the previous subsection as the special case of pure diffusion, the Fourier synthesis is shown of the modes determined from the computations described in the preceding paragraph. As noted before, the plot is shown in a coordinate system representing either the Lagrangian or Eulerian systems, since they are the same when the Reynolds number is zero.

In Figure 6 the Fourier amplitudes for modes 1, 3, 5 and 7 are shown in the same order as in Figure 5, but for a Reynolds number of 2 and all else the same as described for the calculation shown in Figure 3. The first difference to note is that the Fourier amplitudes are complex in this case.

Also, the mode amplitudes are developing an oscillatory nature for small values of η, in contrast to the case of zero Reynolds number.

In Figure 7 is shown the Fourier synthesis in Lagrangian coordinates of the mode amplitudes from the calculation shown in the previous figure. The flame sheet has been designated to be at $Z = 1/2$ and contours of constant Z for $Z > 1/2$ are shown as solid lines whereas contours of constant Z for $Z < 1/2$ are dashed lines. Note that the contours approach straight lines away from the origin, but close to the origin diffusion is winding up the contours in the direction opposite to the rotation (the rotation due to the vortex is counterclockwise).

In Figure 8 is shown the corresponding plot of constant-Z contours in the Eulerian coordinate system. It is interesting to note that the contours are distorted by the convective winding of the vortex, but that near the origin, there is much less winding than in the Lagrangian coordinate system.

3.5 Large-Schmidt-Number Analytical Results

The numerical computations become increasingly difficult as the Reynolds number is raised both because the convective mixing becomes more convoluted within a specified radius and because the radial distance over which the calculations must be carried for a particular accuracy must be substantially increased. Therefore, the large Schmidt number analysis is very useful for examining the structure of the solution for large Reynolds number. Again, this is also a quite realistic assumption for diffusion-controlled reactions in miscible liquids.

In Figure 9 is shown plots of the interface shape calculated from the large Schmidt number analysis for three values of the Reynolds number, 1, 10 and 100, in a Lagrangian coordinate system; these plots have been calculated for a Schmidt number of 10, which satisfies the requirements of the analysis presented in Subsection 3.2 that the Schmidt number be large. These plots have the same scale, so that structures formed at larger Reynolds number extend to larger radius (or similarity variable η). For Reynolds number of unity, in Lagrangian coordinates, the interface hardly varies from a straight line. The circle around the origin shows the radius at which the burnt core is located (the location at which the amplitudes in

Eq.(18) are down from the value 1/2 by $\exp(-3)$). The two plots for larger Reynolds numbers, 10 and 100, show increased distortion of the interface around the origin and growth of the circle representing the burnt core. The distortion of the interface is in the direction opposite to that of the convective mixing, which is positive in the counterclockwise direction, as noted in the discussion of the numerical results in the last subsection. As noted there, this is because the mixing increases the gradients between fuel and oxidizer, enhancing counterrotation diffusion. Note furthermore that the deviations of the interface from planar outside of the burnt core is very small, showing that beyond the burnt core the interface between fuel and oxidizer is essentially controlled by the convective mixing.

In Figure 10 is shown plots of the interface shape in Eulerian coordinates for the same three values of Reynolds number and for the Schmidt number shown in Figure 9. These plots are drawn approximately to scale, so that structures formed at larger Reynolds number extend to larger radius (or similarity variable η). In each plot the area has been blackened within the burnt core to indicate no reaction activity. As in Figure 9, the burnt core grows with increasing Reynolds number. Once again it should be emphasized that these plots do not represent time evolution, but rather different parametric configurations; time evolution is according to the similarity laws determined by the similarity variable $\eta = r^2/4\pi t$. The amount of convective mixing in the counterclockwise direction increases dramatically with Reynolds number; both the radial distance from the origin at which the interface deviates from planar and the winding of the interface inside of this radial location are substantially larger for $\mathrm{Re} = 100$ than for $\mathrm{Re} = 10$.

4 Consumption Rate

Important quantities of interest from this analysis are the global consumption rates for fuel and oxidizer and the global rate of heat release; it is desired to calculate these quantities as functions of the Reynolds number, Schmidt number and initial concentrations of fuel and oxidizer. The consumption rates under general conditions can be calculated from the analysis presented earlier but require computation of Fourier amplitudes using an

ODE solver, synthesis of the solution using FFT routines, location of the flame surface using a root finder and integration over the whole sheet to obtain the global rates.

The local rates of consumption of fuel and of oxidizer and the rate of heat release are all proportional to the derivative of Z normal to the flame surface. Therefore, the calculation of these quantities requires us first to locate the flame sheet and then to determine the derivative of the Z normal to it. When the Schmidt number is large, the analytical results of Subsection 3.2 can be used both to locate the flame sheet and to obtain an expression for the normal derivative of Z. When the initial mixture of fuel and oxidizer is stoichiometric, the flame sheet occurs at $Z = 1/2$ and is located along the curves determined in Lagrangian coordinates by $\Phi_0 = 0$ (Eqs.(19)):

$$\theta_0 = \pm\frac{\pi}{2} + \frac{\mathrm{Re}}{2\,\mathrm{Sc}}\tilde{f}_2(\eta) \tag{20}$$

These lines are transformed by Eqs.(4) into the Eulerian system:

$$\theta = \pm\frac{\pi}{2} + \frac{\mathrm{Re}}{2\,\mathrm{Sc}}\tilde{f}_2(\eta) + \frac{\mathrm{Re}}{2\eta}\left[1 - E_2(\eta)\right] \tag{21}$$

The flame sheet then consists of two curves each of the form $\theta(\eta)$.

The tangent and the normal to the curve defining the flame sheet are given by the expressions

$$\vec{t} = \frac{\vec{i}_r + \vec{i}_\theta r\frac{d\theta}{dr}}{\sqrt{1 + \left(\frac{d\theta}{dr}\right)^2 r^2}} \qquad \vec{n} = \frac{-r\frac{d\theta}{dr}\vec{i}_r + \vec{i}_\theta}{\sqrt{1 + \left(\frac{d\theta}{dr}\right)^2 r^2}} \tag{22}$$

where, from Eq.(21),

$$r\frac{d\theta}{dr} = \mathrm{Re}\,\eta\frac{d}{d\eta}\left[\frac{\tilde{f}_2(\eta)}{\mathrm{Sc}} + \frac{1 - E_2(\eta)}{\eta}\right] \tag{23}$$

or

$$r\frac{d\theta}{dr} = \left(\frac{\mathrm{Re}}{\mathrm{Sc}}\left[\frac{1 - 2E_3(\eta)}{\eta^2} - \frac{2E_2(\eta)}{\eta} - E_1(\eta)\right] - \frac{1 - E_2(\eta)}{\eta} + E_1(\eta)\right) \tag{24}$$

The gradient of Z in cylindrical coordinates, $\vec{i}_r \partial Z/\partial r + (\vec{i}_\theta/r)\partial Z/\partial\theta$, can be found in Lagrangian coordinates using Eq.(4) and then in terms of the similarity variables $\eta = r^2/(4\nu t), \theta_0$ (where we note that the Lagrangian variables ρ and τ can be replaced by r and t):

$$\nabla Z = \frac{1}{r}\left[2\eta\frac{\partial Z}{\partial \eta} + \mathrm{Re}\,\frac{1-\exp(-\eta)}{\eta}\frac{\partial Z}{\partial \theta_0}\right]\vec{i}_r + \frac{1}{r}\frac{\partial Z}{\partial \theta_0}\vec{i}_\theta \tag{25}$$

The analytical expression Eq.(18) for $\tilde{Z}$ can be differentiated and evaluated along the flame sheet $\Phi_0 = 0$. When this is done, we find

$$\begin{aligned}\frac{\partial \tilde{Z}}{\partial \eta} &= \left(-\frac{\mathrm{Re}}{2\,\mathrm{Sc}}\frac{d\tilde{f}_2}{d\eta}\right)\frac{\partial \tilde{Z}}{\partial \theta_0} \\ \frac{\partial \tilde{Z}}{\partial \theta_0} &= \pm\frac{2}{\pi}\sum_{m=0}^{\infty}\exp\left(-\frac{(2m+1)^2}{4\,\mathrm{Sc}\,\eta}\left[1+\mathrm{Re}^{\,2}\tilde{f}_1(\eta)\right]\right)\end{aligned} \tag{26}$$

Finally, the consumption rates of fuel and oxidizer locally are

$$dC = D\frac{dZ}{dn}ds = D\vec{n}\cdot\nabla Z\,ds \tag{27}$$

where D is the species diffusion coefficient, $\vec{n}$ is the normal direction to the flame sheet, and s is the arc length along the flame sheet. Here

$$ds = \sqrt{1 + r^2\left(\frac{d\theta}{dr}\right)^2}\,dr \tag{28}$$

Then the total consumption rate for either species is

$$C = D\int_{flamesheet}\frac{dZ}{dn}ds \tag{29}$$

One additional complication arises at this point. In the case when there is no vortex imposed on the reaction process, i.e. in the pure diffusion case, the consumption rate is infinite because there is an infinitely long flame length over which the reaction takes place. When the vortex is imposed, the reaction rate is still infinite because there is also an infinite flame length beyond the region influenced by the vorticity. Therefore, we determine the

enhancement caused by the imposition of the vortex. If we denote by C_0 the consumption rate in the pure diffusion case ($\mathrm{Re} = 0$), then we desire $C - C_0$.

Calculation of the consumption rate enhancement at this point would require numerical integration. In an attempt to push the analytical calculations as far as possible and to obtain expressions with which to compare with those derived by Marble and Karagozian [14], [23] [24], we further assume that the Reynolds number is large. A large Reynolds number is one for which the functions $\tilde{A}_m(\eta; \mathrm{Re}, \mathrm{Sc})$ appearing in the exponential amplitudes in the asymptotic solution Eq.(18) are large enough that these amplitudes are small; then the terms in the Fourier series decrease very rapidly with increasing m and for our purposes, the Fourier series can be approximated by only one term. Therefore, for $m = 1$, we require that $\tilde{A}_1 \geq 3$ approximately; a Reynolds number of 100 or more is adequate for example. Then, the asymptotic expressions for $\tilde{f}_1$ and $\tilde{f}_2$ for large η ,which were given earlier, can be used. Using only the first term in the Fourier series solution Eq.(18) and taking only the "large η" expression for the equation for the flame sheet and for the Eulerian-Lagrangian transformation, we find

$$r\frac{d\theta}{dr} \approx -\frac{\mathrm{Re}}{\eta}\left(1 - \frac{1}{2\,\mathrm{Sc}}\right) \tag{30}$$

and

$$\frac{d\tilde{Z}}{dn}ds \approx \frac{1}{\pi}\exp\left[-\frac{1}{4\,\mathrm{Sc}\,\eta}\left(1 + \frac{\mathrm{Re}^2}{3\eta^2}\right)\right]d\eta \tag{31}$$

Integration of the approximate expression for the local enhancement of the consumption rate over the flame sheet, then gives the global enhanced species consumption rate:

$$C - C_0 \approx \frac{\tilde{\Gamma}(2/3)}{\pi} D\left(\frac{2\,\mathrm{Re}^2\,\mathrm{Sc}^2}{3}\right)^{1/3} \tag{32}$$

and the parametric dependence of this expression agrees with that reported by Marble and Karagozian [14], [23], [24].

5 Conclusions

As noted earlier, this problem was originally formulated by F. Marble and analyzed by Marble and Karagozian [14],[23] using solutions developed by Carrier et al. [15], which are valid locally along the flame sheet. In this paper we analyze the same problem by alternate methods, ones that accurately solve the equations globally. In particular, the Marble problem has no natural length nor time scale associated with it, and, therefore, allows a global similarity solution, an observation which reduces the number of dependent variables from three (radius, angle and time) to two (angle and the similarity variable - which has the character of similarity variables for diffusion processes). Perhaps the most important analytical result is that which expresses the dependence of the species consumption rate on the Reynolds and Schmidt numbers for large values of these parameters, and this result corroborates that found by Marble [14].

The solution presented here elucidates, we believe, the nature of the problem, and the method of solution provides all of the machinery necessary to calulate additional results to whatever accuracy one might desire for other purposes, such as comparing with more general numerical solutions [16]-[21]. The key features of the analysis are the observations that the problem permits a global similarity solution and that the equations can be transformed to Lagrangian coordinates. The first observation reduces the number of independent variables from three to two, and the second eliminates scaling difficulties arising in convection-diffusion equations when the Reynolds number is large. The Marble problem is inherently interesting because it addresses the question of enhancement of species consumption and heat release rates by flame stretching in a simple geometry. It is also of interest because, as discussed earlier, it simulates the enhancement in these rates in a vortex generated in a two dimensional shear layer [9]-[12].

The Marble problem can clearly be extended in several directions. Obvious directions for generalization are to consider other flow fields, more general geometries for the initial fuel and oxidizer configurations, and the effects of density changes induced by heat release on mixing. A more general flow field and density variations have been considered analytically by Karagozian and Marble [23],[24], using the same type of local analysis orig-

inally employed by Marble. A more general flow and generalized species geometries are investigated analytically in the paper by Baum et al. [13]; a three dimensional flow field consisting of a stretched vortex is considered, a very important generalization for turbulence where vortex stretching is crucial. Finite regions of fuel in an oxidizing atmosphere, e.g. a sphere of fuel in an oxidizing background, are also a practical generalization considered in the paper of Baum et al. These generalizations are also the subject of investigation by numerical techniques [16]-[21].

Finally, the work presented here can be viewed in a larger context, where it, or its generalization, is regarded as a submodel of a more general model for turbulent combustion. The large scale fluid motion for whatever geometry must be computed in a large Reynolds number or essentially inviscid approximation. We have developed such a large scale model for buoyant convection induced by a room fire [25], [26],[27]. However, the large scale flow could as well be calculated for other configurations, and then the small scale combustion submodel would be embedded into this flow field.

We wish to thank Dr. G.B. McFadden for a useful discussion and commments on the paper and Dr. C. Fenimore for helpful comments on the paper. This research was partially supported by the Air Force Office of Scientific Research under Contract AFOSR-ISSA-87-0018.

References

[1] Libby, P.A. and Williams, F.A. (eds), *Turbulent Reacting Flows*, Springer-Verlag, Berlin, 1980.

[2] Williams, F.A., *Combustion Theory, The Fundamental Theory of Chemically Reacting Flow Systems*, Second Edition, The Benjamin/Cummings Publishing Co., Inc., Menlo Park, California, 1985.

[3] Buckmaster, J.D. and Ludford, G.S.S., *Theory of Laminar Flames*, Cambridge University Press, 1982.

[4] Buckmaster, J.D. and Ludford, G.S.S., *Lectures on Mathematical Combustion*, Society for Industrial and Applied Mathematics, Philadelphia,

Pennsylvania, 1983.

[5] Oran, E.S. and Boris, J.P., Detailed Modelling of Combustion Systems, *Prog. Energy Combust. Sci.*, Vol. 7, 1981, pp 1-72.

[6] Peters, N., "Laminar Diffusion Flamelet Models in Non-Premixed Turbulent Combustion", *Prog. Energy Combust. Sci.*, Vol. 10, 1984, pp 319-339.

[7] Oppenheim, A.K., "The Beauty of Combustion Fields and Their Aerothermodynamic Significance", *Dynamics of Reactive Systems Part I: Flames and Configurations*, J.R. Bowen, J.-C. Leyer and R.I. Soloukhin (eds), Progress in Astronautics and Aeronautics, Vol 105, 1986, A.I.A.A., 1633 Broadway, N.Y.,N.Y. 10019.

[8] Ashurst, W.T., "Vortex Simulation of Unsteady Wrinkled Laminar Flames", *Combust. Sci. Technology*, Vol. 52, 1987, p 325.

[9] Brown, G.L. and Roshko, A., "On Density Effects and Large Structure in Turbulent Mixing Layers", *J. Fluid Mech.*, Vol. 91, 1974, pp 319-335.

[10] Roshko, A., "Structures of Turbulent Shear Flows: A New Look", *A.I.A.A. Journal*, Vol.14, 1976, pp 1349-1357.

[11] Mungal, M.G. and Dimotakis, P.E., "Mixing and Combustion with Low Heat Release in a Turbulent Shear Layer", *J. Fluid Mech.*, Vol. 148, 1984, pp 349-382.

[12] Browand, F.K., "The Structure of the Turbulent Mixing Layer", *Physica* Vol 18D, 1986, pp 135-148.

[13] Baum, H.R., Corley, D.M. and Rehm, R.G. "Time-Dependent Simulation of Small-Scale Turbulent Mixing and Reaction", Paper presented at the Twenty-First International Symposium on Combustion, Munich, West Germany, August 3-8, 1986.

[14] Marble, F.E. "Growth of a Diffusion Flame in the Field of a Vortex", *Recent Advances in Aerospace Sciences* (C. Cassci, Ed.) 1985, p.315.

[15] Carrier, G.F., Fendell, F.E. and Marble, F.E., "The Effect of Strain Rate on Diffusion Flames", *SIAM J. Appl. Math.*, Vol.28, No. 2, March, 1975.

[16] Riley, J.J., Metcalfe, R.W. and Orszag, S.A., "Direct Numerical Simulations of Chemically Reacting Mixing Layers", *Phys. Fluids*, Vol. 29, 1986, pp 406-422.

[17] McMurtry, P.A., Jou, W.-H., Riley, J.J. and Metcalfe, R.W., "Direct Numerical Simulations of a Reacting Mixing Layer with Chemical Heat Release", *A.I.A.A. Journal*, Vol 24, 1986, pp 962-970.

[18] McMurtry, P.A. and Riley, J.J., "Mechanisms by Which Heat Release Affects the Flow Field in a Chemically Reacting, Turbulent Mixing Layer", Paper AIAA-87-0131, paper presented at the AIAA 25th Aerospace Sciences Meeting, January 12-15, 1987, Reno, Nevada.

[19] McMurtry, P.A., "Direct Numerical Simulations of a Reacting Mixing Layer with Chemical Heat Release", Ph.D. Thesis, Mechanical Engineering, University of Washington, Seattle, Washington, 1987.

[20] Ghoniem, A.F. and Givi, P., "Vortex-Scalar Element Calculations of a Diffusion Flame", Paper AIAA-87-0225, paper presented at the AIAA 25th Aerospace Sciences Meeting, January 12-15, 1987, Reno, Nevada.

[21] Laverdant, A.M. and Candel, S.M. "A Numerical Analysis of a Diffusion Flame-Vortex Interaction", Paper presented at the SIAM Conference on Numerical Combustion, San Francisco, California, March 9-11, 1987.

[22] Rehm, R.G., Baum, H.R. and Lozier, D.W. "Two-Dimensional Flame in a Vortex Field", Paper presented at the SIAM 1986 National Meeting, Boston, Mass. July 21-25, 1986.

[23] Karagozian, A.R. and Marble, F.E., "Study of a Diffusion Flame in a Stretched Vortex", *Comb. Sci. Tech.*, Vol. 45, 1986.

[24] Karagozian, A.R., "An Analytical Study of Diffusion Flames in Vortex Structures", Ph.D. Thesis, California Institute of Technology, Pasadena, Cal., 1982.

[25] Rehm, R.G. and Baum, H.R., "The Equations of Motion for Thermally Driven, Buoyant Flows", *J. Research Nat. Bur. Standards*, Vol. 83, 1978, pp 297-308.

[26] Baum, H.R., Rehm, R.G., Barnett, P.D. and Corley, D.M., " Finite Difference Calculations of Buoyant Convection in an Enclosure, I. The Basic Algorithm", *SIAM J. Sci. Stat. Comput.*, Vol. 4, 1983, pp 117-135.

[27] Baum, H.R. and Rehm, R.G., "Calculations of Three Dimensional Buoyant Plumes in Enclosures", *Comb. Sci. Tech.*, Vol. 40, 1984, pp 55-77.

Figure Captions

1. Schematic diagram of the Marble problem. Fuel, in the shaded left half-plane, and oxidizer in the right are allowed to react at the thin flame sheet separating them. Simultaneously, a line vortex with its axis at the origin induces convective mixing between the two species. The objective is to calculate the enhancement of the species consumption caused by the mixing.

2a. Function $\tilde{f}_1(\eta)$ defined following Eq.(19); the function arises in the large Schmidt number asymptotic analysis.

2b. Function $\tilde{f}_2(\eta)$ defined following Eq.(19); the function arises in the large Schmidt number asymptotic analysis.

3. Contours of constant species concentration (constant Z) for pure diffusion. In this special case the vorticity is zero so that $\Gamma = 0$ and $\mathrm{Re} = 0$, and, therefore, there is no convective mixing. The contours should be straight lines (distorted by the plotting routines) with the species concentrations changing in a one-dimensional fashion from the initial concentration of fuel on the left to the initial concentration of oxidizer on the right. The flame sheet could be located along any one of these contours depending upon these initial concentrations; in this plot a stoichiometric mixture existed initially and the flame sheet occurs along the initial interface with constant-density fuel contours shown by solid lines and constant-density oxidizer lines dashed. Contours are not shown all of the way to the origin, and a horizontal solid line is shown for technical reasons.

4. The interface between fuel and oxidizer for four values of the Reynolds number, $\mathrm{Re} = 2, 4, 6$ and 8, when there is no diffusion ($D = 0$ and $\mathrm{Sc} = \infty$): Reynolds number increases from top to bottom. These plots illustrate the convective mixing induced by the vorticity and show that the mixing is enhanced as the Reynolds number is increased.

5. Numerical solutions to Eqs.(5) for four mode amplitudes, modes 1, 3, 5 and 7, as functions of the similarity variable η for Reynolds number zero and Schmidt number one and a stoichiometric mixture. Mode 1 is in the upper left corner, mode 3 in the upper right, mode 5 in the lower left and mode 7 in the lower right. The solid curve is the real part of the mode amplitude, the dashed curve is the imaginary part and the asterisks curve is the modulus. Since this is the pure diffusion case, the amplitudes are real. There were 99 integration nodes used for the calculation.

6. Numerical solutions to Eqs.(5) for four mode amplitudes, modes 1, 3, 5 and 7, as functions of the similarity variable η for Reynolds number two and Schmidt

number one and a stoichiometric mixture. All other conditions are the same as those in Figure 5.

7. Solution of Eq.(2) in the Lagrangian coordinate system for a stoichiometric mixture, a Reynolds number of two and a Schmidt number of unity. This solution is found using Fourier synthesis of 15 modes of which four are shown in Figure 6. Contours of constant fuel density are shown as solid curves while contours of constant oxidizer are dashed; the flame sheet occurs at the solid curve which divides fuel and oxidizer regions. Note that the contours approach straight lines away from the origin, and close to the origin, diffusion induces counterclockwise gradients (opposite to the clockwise mixing of the vortex).

8. Solution of Eq.(2) in the Eulerian coordinate system for the case shown in Figure 7. In this coordinate system, the contours are distorted by the convective winding of the vortex, but near the origin, there is much less winding than in the Lagrangian system.

9. Plots of the interface shape for three values of the Reynolds number, 1, 10 and 100, in a Lagrangian coordinate system as determined by the large Schmidt number asymptotic analysis: these plots were calculated for a Schmidt number of 10, which satisfies the requirements of this analysis. The circle around the origin shows the radius at which the burnt core is located as discussed in the text.

10. Plots of the interface shape in Eulerian coordinates for the same conditions shown in Figure 9. In each plot, the area within the burnt core has been blackened. The amount of convective mixing and the distance from the origin at which the interface deviates from planar increases dramatically with Reynolds number.

Vortex, Flame-Sheet Interaction

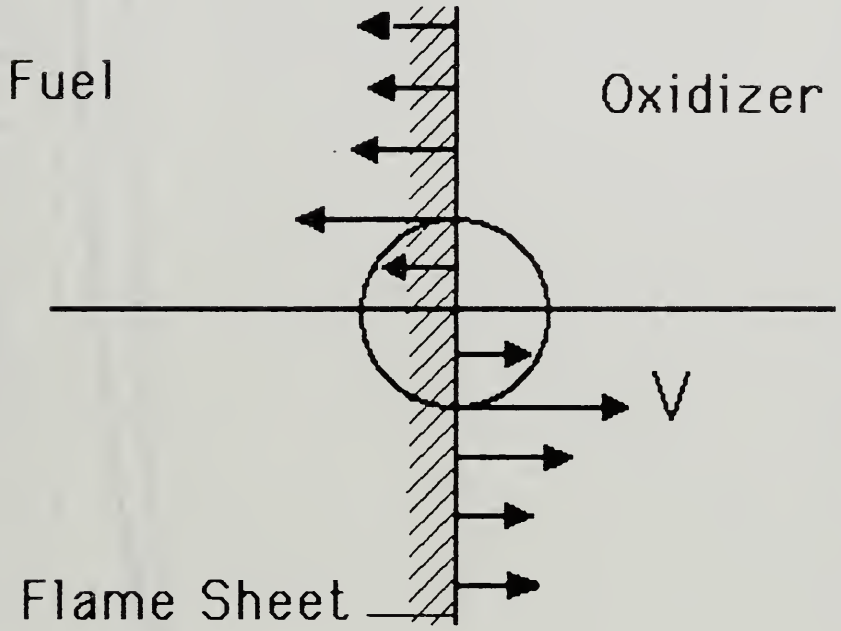

Figure 1

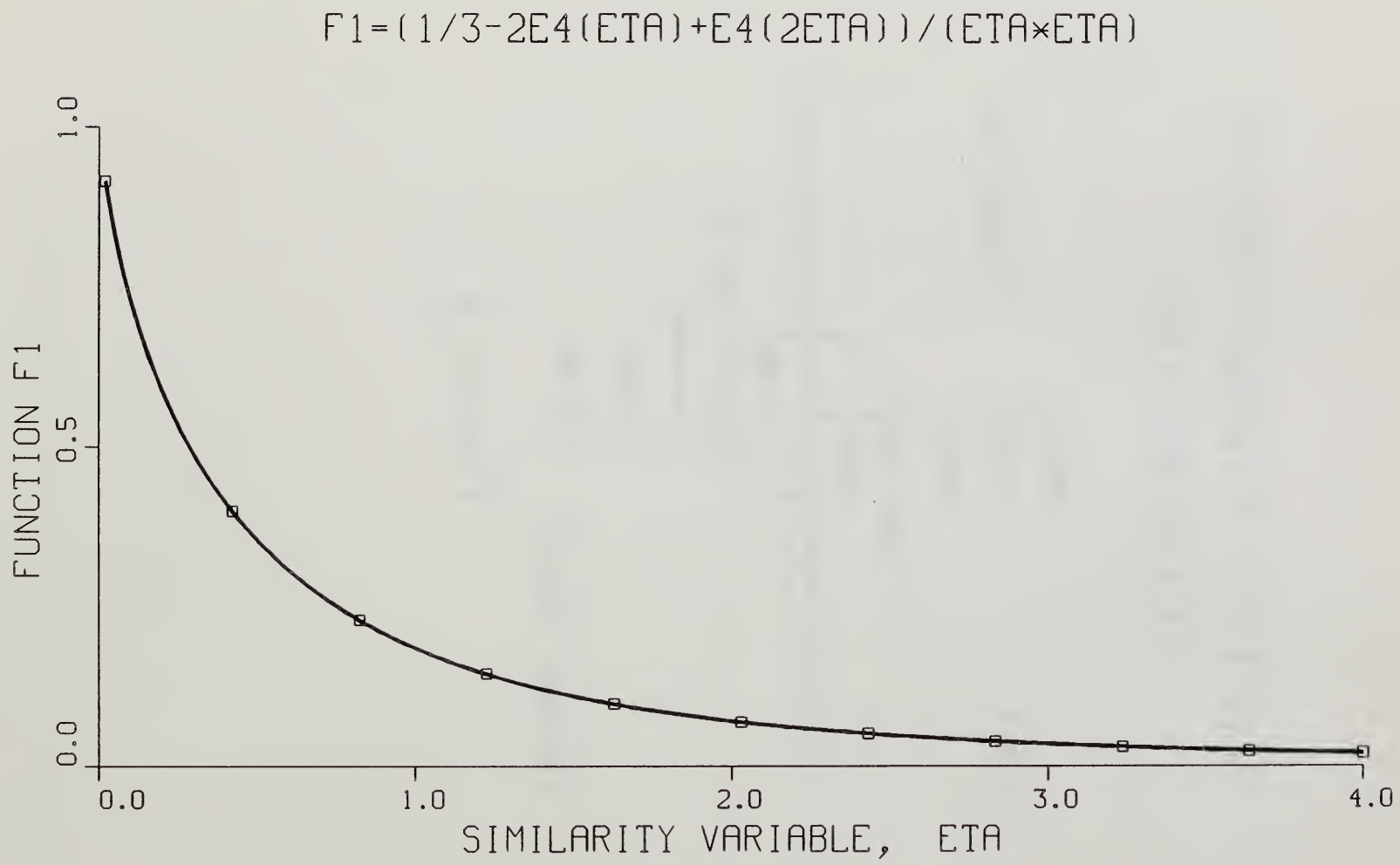
F1=(1/3-2E4(ETA)+E4(2ETA))/(ETA*ETA)
FUNCTION F1
1.0
0.5
0.0
0.0
1.0
2.0
3.0
4.0
SIMILARITY VARIABLE, ETA

Figure 2a

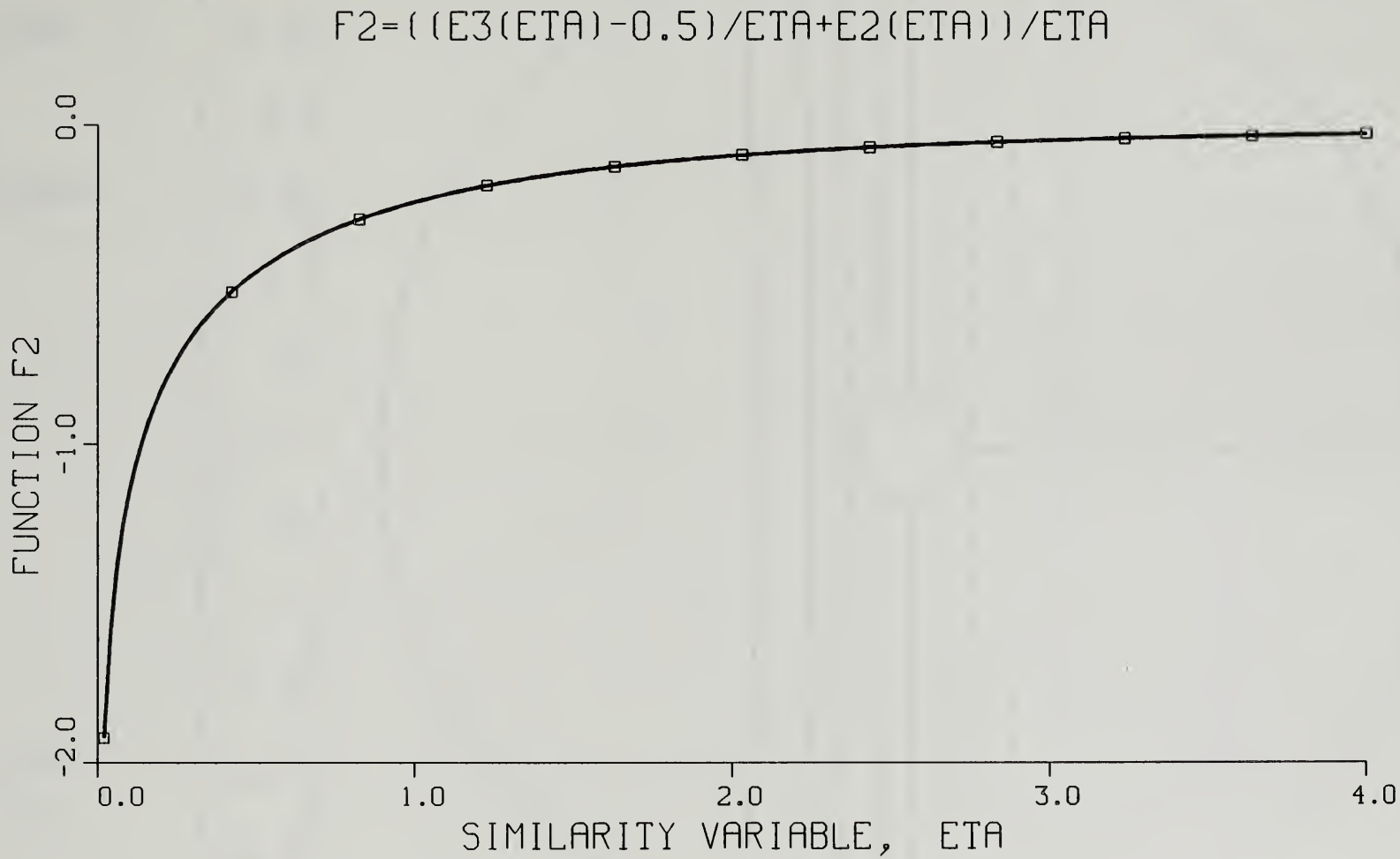
F2=((E3(ETA)-0.5)/ETA+E2(ETA))/ETA
FUNCTION F2
0.0
-1.0
-2.0
0.0
1.0
2.0
3.0
4.0
SIMILARITY VARIABLE, ETA

Figure 2b

LAGRANGIAN
COORDINATES

FLAME SUR-
FACE CONTOUR
- .5

REYNOLDS
NUMBER
- 0.

SCHMIDT
NUMBER
- 1.

NMODES - 15
NPTS - 99
CROSS - 1.
TRUNC - 10.

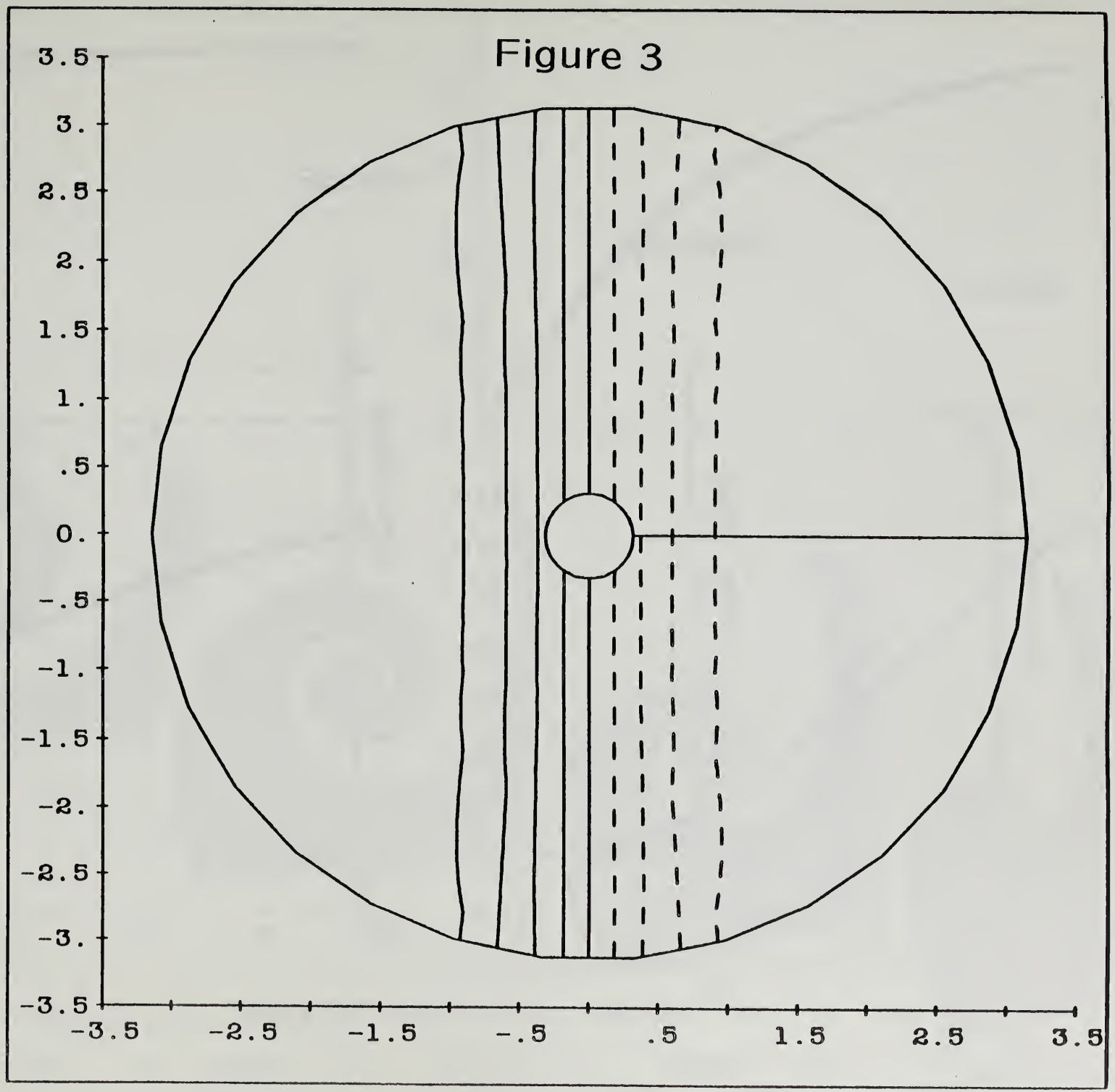

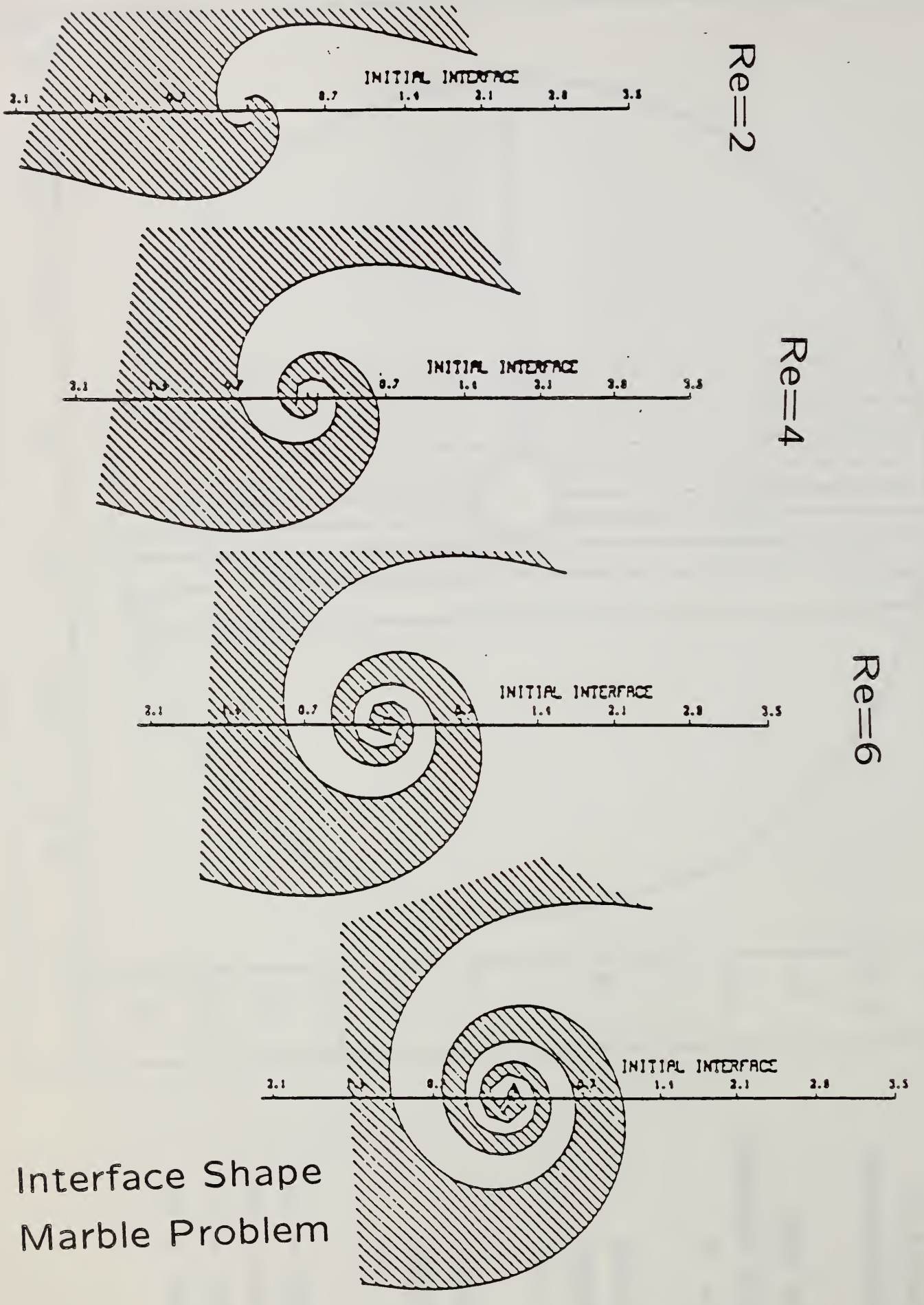

Interface Shape
Marble Problem

Figure 4

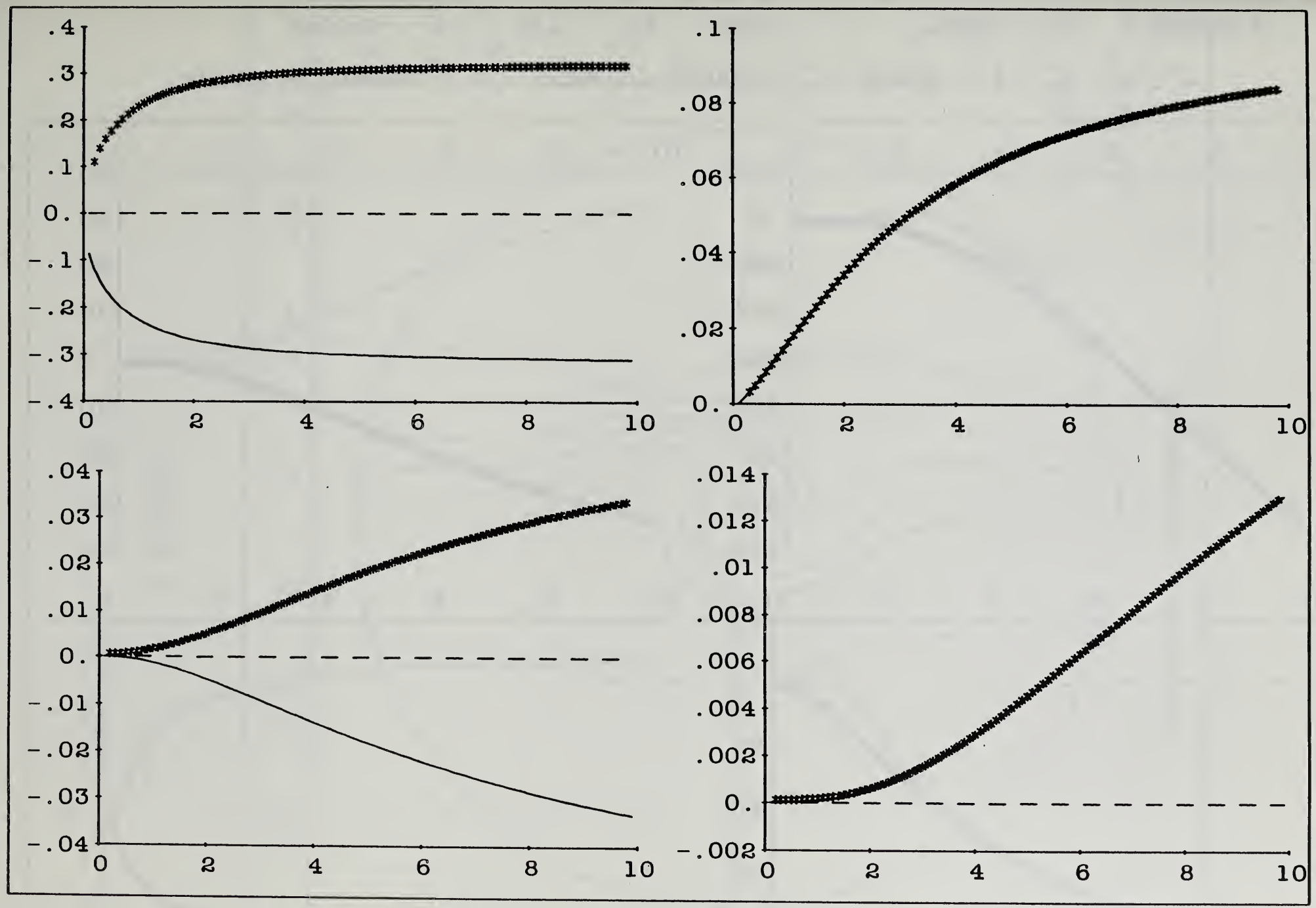

REYNOLDS NUMBER = 0. SCHMIDT NUMBER = 1. MODES 1 3 5 7

NMODES - 15 NPTS - 99 CROSS - 1. TRUNC = 10.

Figure 5

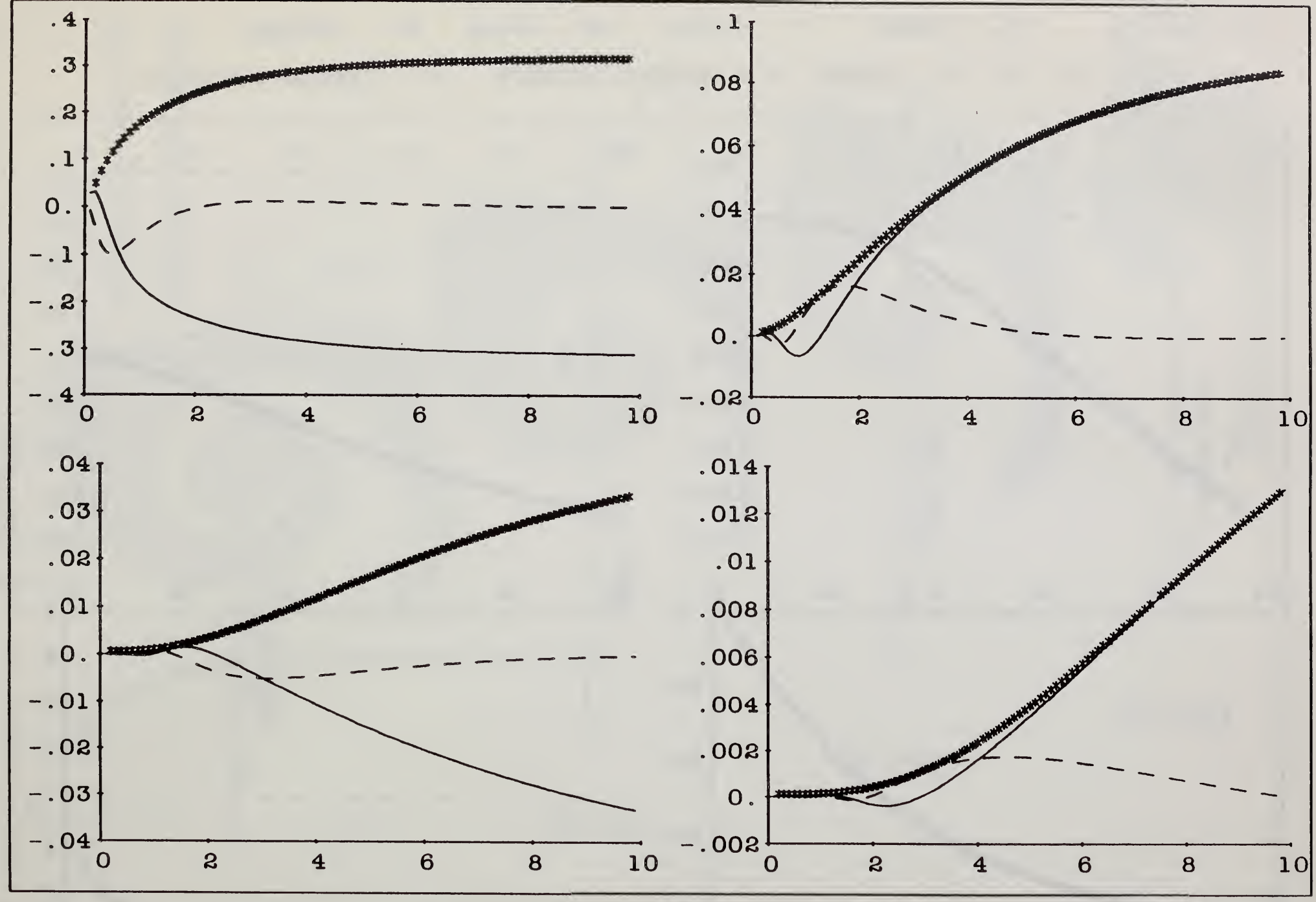

REYNOLDS NUMBER = 2. SCHMIDT NUMBER = 1. MODES 1 3 5 7

NMODES = 15 NPTS = 99 CROSS = 1. TRUNC = 10. Figure 6

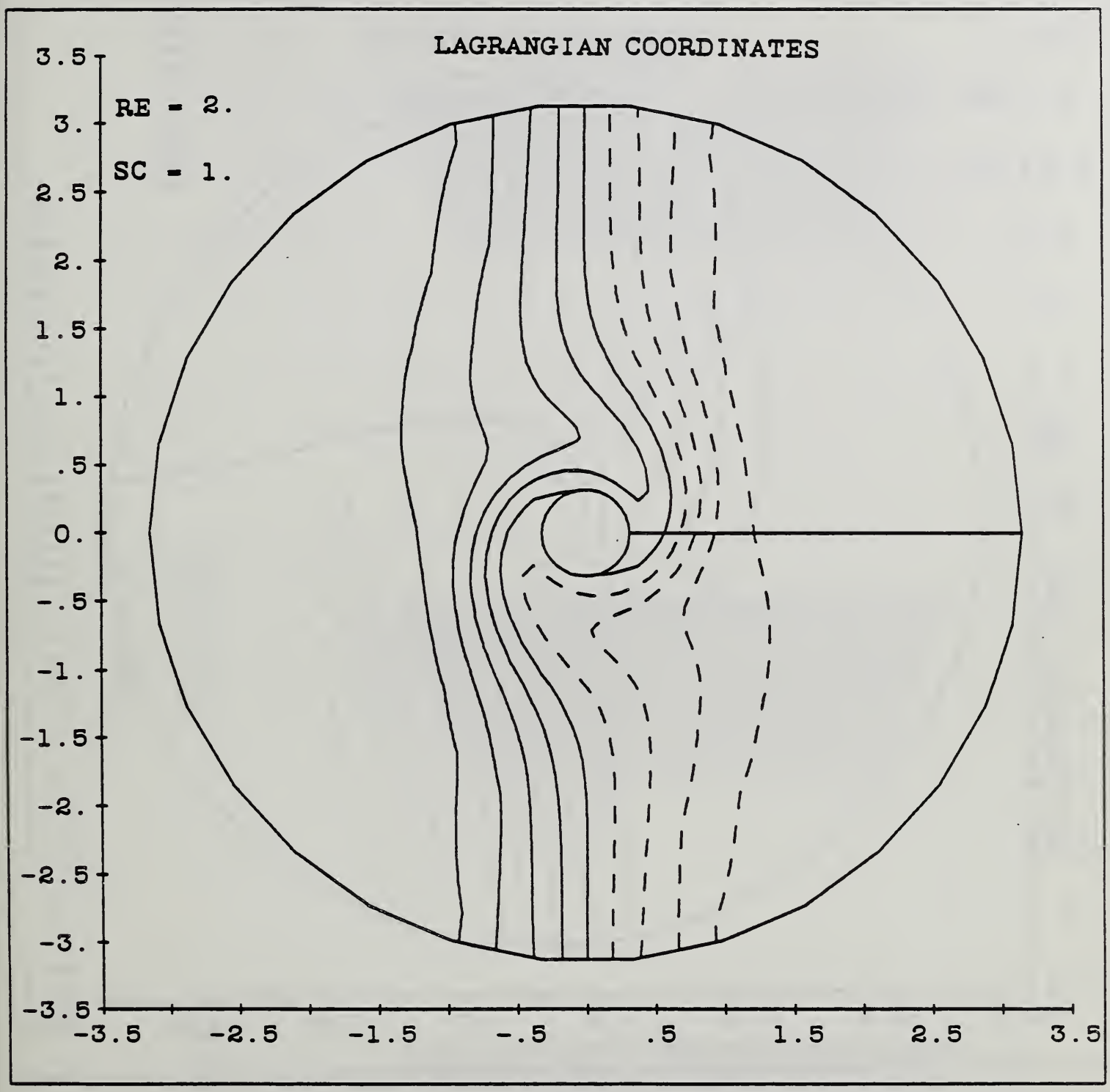
LAGRANGIAN COORDINATES
RE = 2.
SC = 1.
3.5
3.
2.5
2.
1.5
1.
.5
0.
-.5
-1.
-1.5
-2.
-2.5
-3.
-3.5
-3.5
-2.5
-1.5
-.5
.5
1.5
2.5
3.5

Figure 7

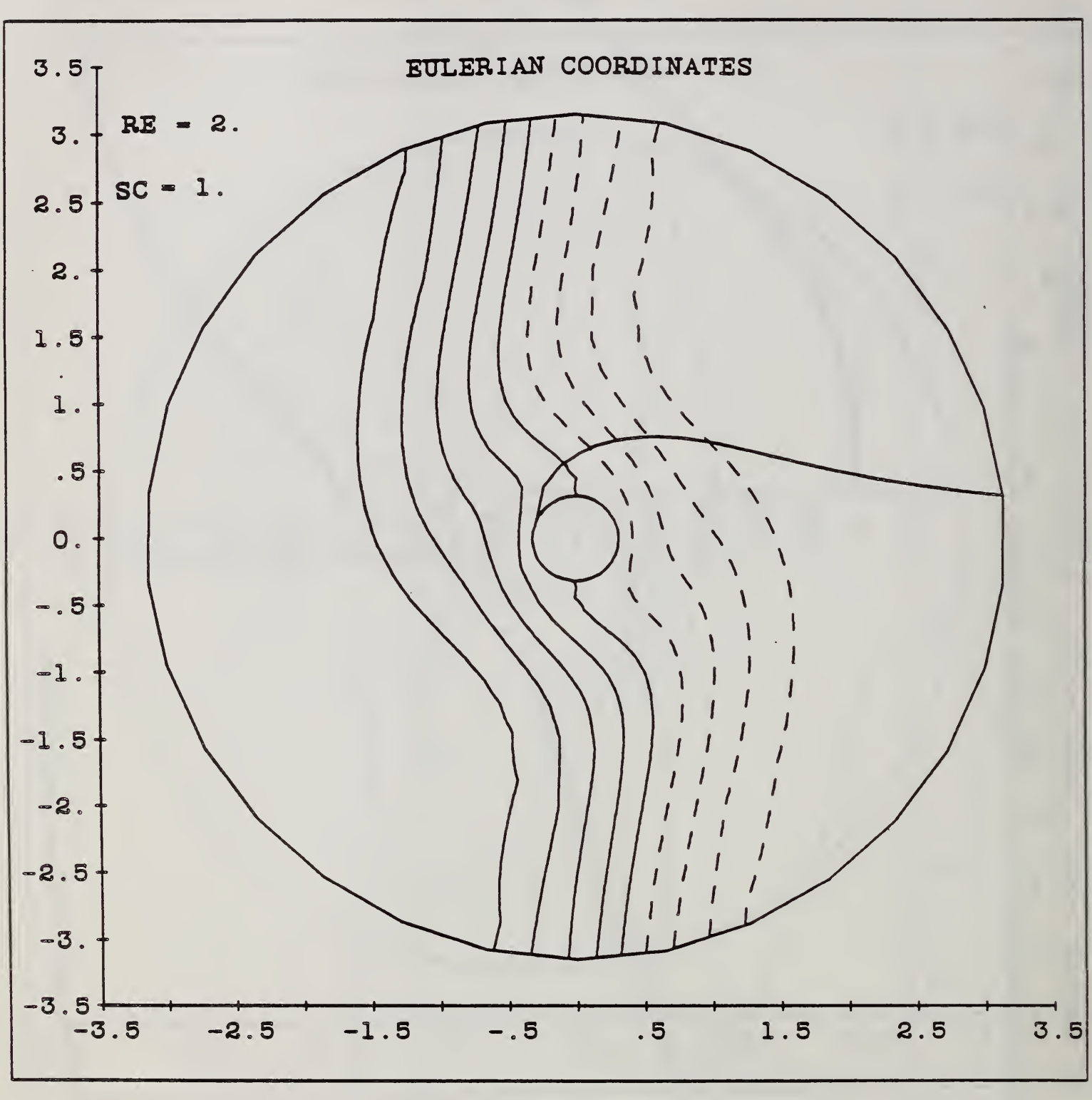
EULERIAN COORDINATES
RE = 2.
SC = 1.
3.5
3.
2.5
2.
1.5
1.
.5
0.
-.5
-1.
-1.5
-2.
-2.5
-3.
-3.5
-3.5
-2.5
-1.5
-.5
.5
1.5
2.5
3.5

Figure 8

Lagrangian Coordinate System

Figure 9

Re=1

Re=10

Re=100

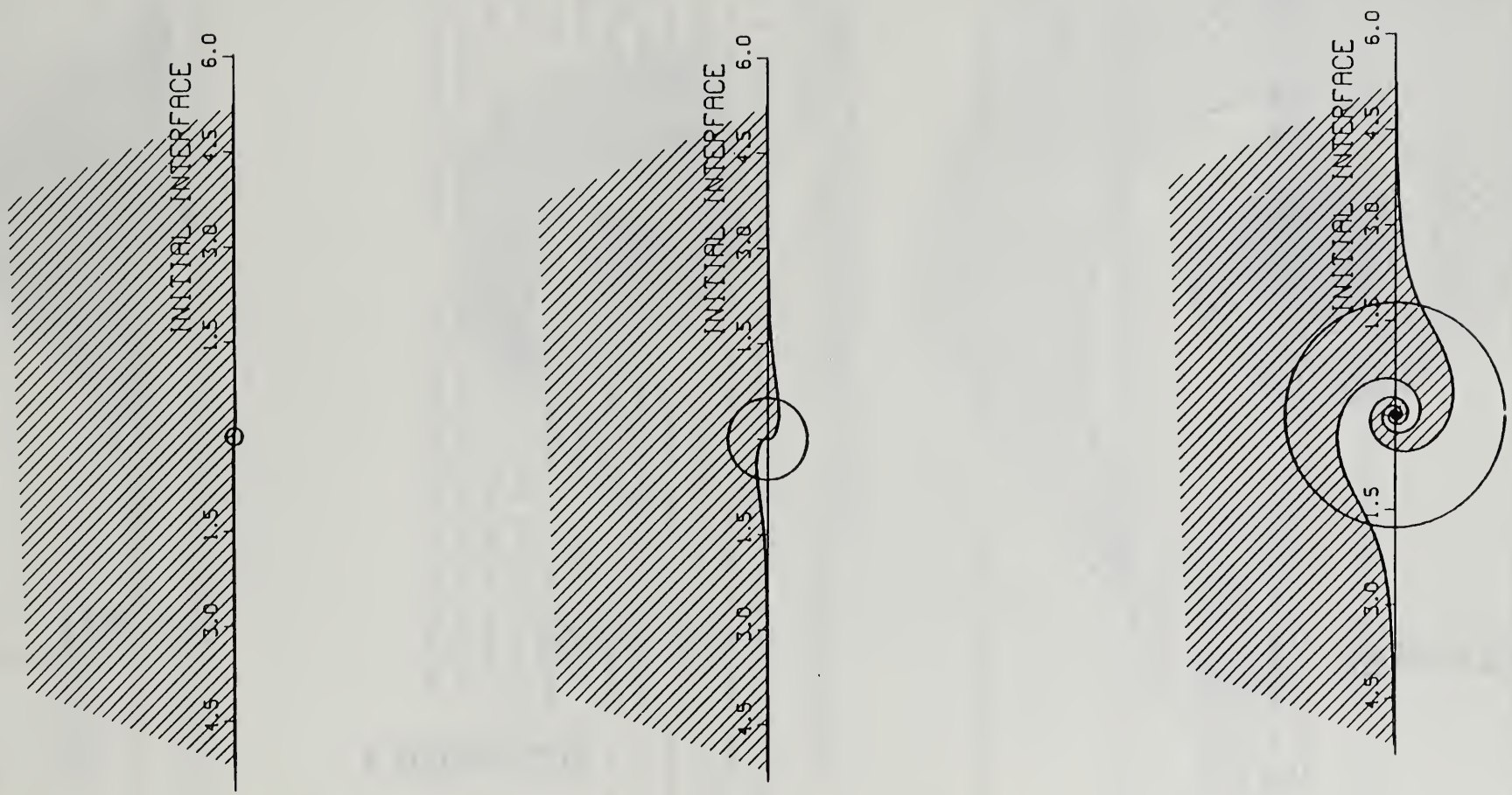

Schmidt No. = 10

Eulerian Coordinate System

Figure 10

Re=1

Re=10

Re=100

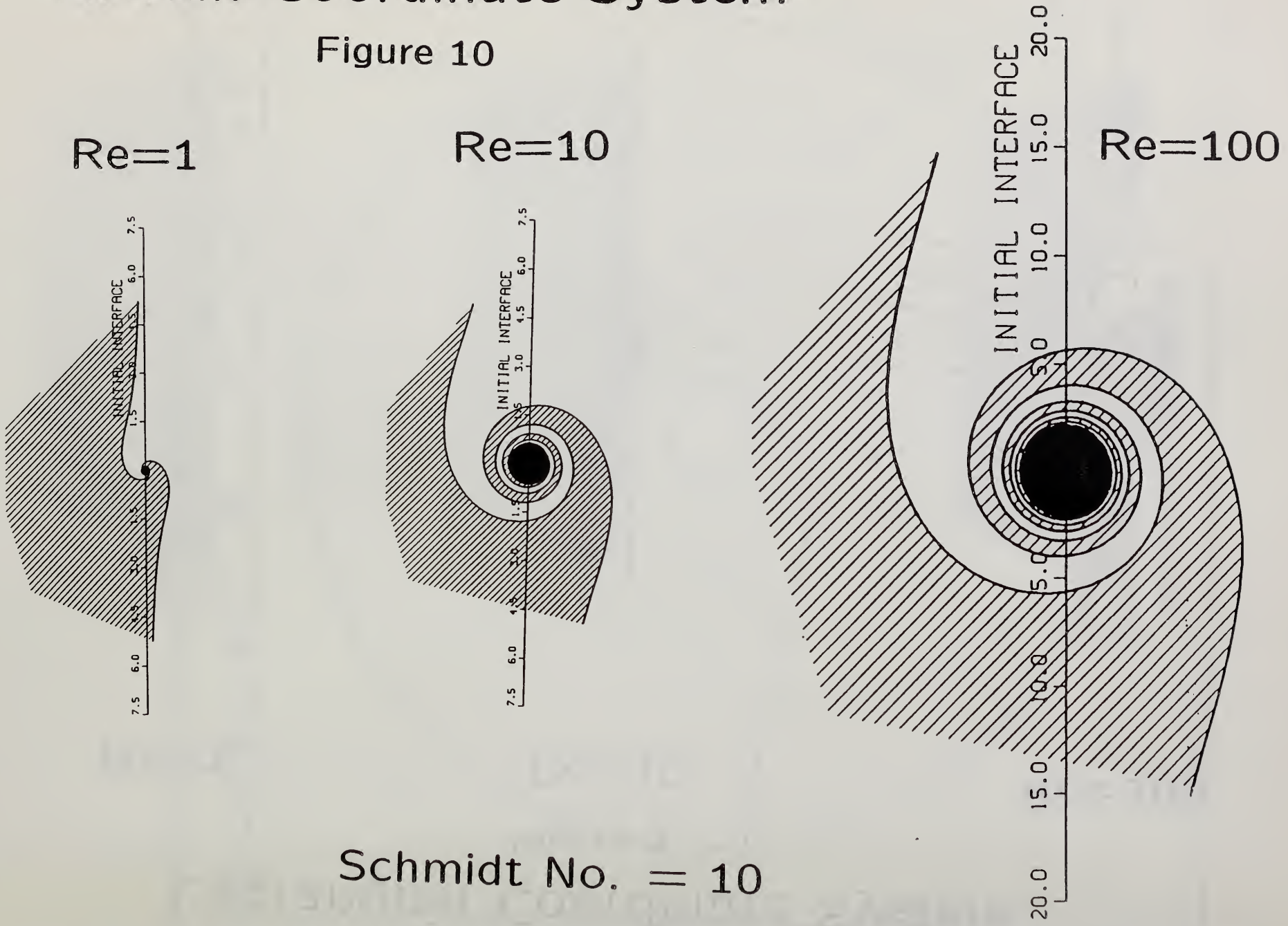

Schmidt No. = 10

NBS-114A (REV. 2-8C)

U.S. DEPT. OF COMM. BIBLIOGRAPHIC DATA SHEET (See instructions)	1. PUBLICATION OR REPORT NO. NBSIR- 87-3572	2. Performing Organ. Report No.	3. Publication Date JUNE 1987

4. TITLE AND SUBTITLE

Diffusion-Controlled Reaction in a Vortex Field

5. AUTHOR(S)

R.G. Rehm, H.R. Baum, and D.W. Lozier

6. PERFORMING ORGANIZATION (If joint or other than NBS, see instructions)

NATIONAL BUREAU OF STANDARDS
DEPARTMENT OF COMMERCE
WASHINGTON, D.C. 20234

7. Contract/Grant No.

AFOSR-155A-87-0018

8. Type of Report & Period Covered

9/86-9/87

9. SPONSORING ORGANIZATION NAME AND COMPLETE ADDRESS (Street, City, State, ZIP)

(Partially supported by)
Air Force Office of Scientific Research
Bolling Air Force Base
Washington, DC 20332

10. SUPPLEMENTARY NOTES

☐ Document describes a computer program; SF-185, FIPS Software Summary, is attached.

11. ABSTRACT (A 200-word or less factual summary of most significant information. If document includes a significant bibliography or literature survey, mention it here)

A two-dimensional model of a constant-density diffusion controlled reaction between unmixed species initially occupying adjacent half-spaces is formulated and analyzed. An axisymmetric viscous vortex field satisfying the Navier-Stokes equations winds up the interface between the species as they diffuse together and react. A flame-sheet approximation of the rapid reaction is made using Shvab-Zeldovich dependent variables. The model was originally proposed by F. Marble, who performed a local analysis and determined the total consumption rate along the flame sheet. The present paper describes a global similarity solution to the problem which is Fourier analyzed in a Lagrangian coordinate system. An asymptotic analysis of the Fourier amplitudes, valid for large Schmidt numbers is presented. The solution is evaluated numerically in Lagrangian and Eulerian coordinate systems. This problem has been studied as part of a more general model which has application to the description of turbulent combustion.

12. KEY WORDS (Six to twelve entries; alphabetical order; capitalize only proper names; and separate key words by semicolons)

combustion; convection; diffusion-controlled; flame-sheet; reaction; turbulent mixing

13. AVAILABILITY

☒ Unlimited

☐ For Official Distribution. Do Not Release to NTIS

☐ Order From Superintendent of Documents, U.S. Government Printing Office, Washington, D.C. 20402.

☒ Order From National Technical Information Service (NTIS), Springfield, VA. 22161

14. NO. OF PRINTED PAGES

40

15. Price

$11.95

USCOMM-DC 6043-P80